Fully gyro-kinetic simulations of Alfvén Eigenmodes in LHD and Geodesic Acoustic Modes in non-axisymmetric geometries

Axel Könies, Alexey Mishchenko, Ralf Kleiber, Matthias Borchardt, Roman Hatzky[1], M. Drevlak, S. Henneberg, J. Geiger, A. Biancalani[1]
Yasushi Todo[2], Donald Spong[3]

Max-Planck-Institut für Plasmaphysik, Wendelsteinstr. 1, D- 17491 Greifswald
[1] Max-Planck-Institut für Plasmaphysik, Boltzmannstr. 2, D- 85748 Garching
[2] National Institute for Fusion ScienceToki, Gifu, 509-5292, Japan
[3] Oak Ridge National Laboratory, Oak Ridge, Tennessee 37831, USA

Dec 13, 2018

This work has been carried out within the framework of the EUROfusion Consortium and has received funding from the European Unions Horizon 2020 research and innovation programme under grant agreement number 633053. The views and opinions expressed herein do not necessarily reflect those of the European Commission.

Introduction

Important Physics to be addressed with gk codes

- fast particle instabilities, redistribution and loss
- W7-X current physics, density profile (low n instablities ?)

EUTERPE

- a number of electro-magnetic calculations for tokamaks: (Mishchenko et al. 2005,2014, 2015 ..., Cole et al. 2015, 2018)
- verification and validation of linear EP physics with GTC, ORB5, GYRO, GEM, MEGA, NOVA-K and FAR on DIII-D successful, (S. Taimourzadeh et al. submitted to Nucl. Fusion)

Introduction

apply fully gyro-kinetic EUTERPE version to Alfvén eigenmodes in LHD

- low mode number, comparison with resistive MHD (MEGA) and gk-electron-fluid (GTC)
- experimental parameters, realistic equilibrium

Geodesic Acoustic Modes in non-axisymmetric geometries

- GAMs are important in tokamaks $\longrightarrow$ this ER project
- GAMs have been studied in LHD $\longrightarrow$ theory (Sugama), experiment
- Strong damping of GAMs in standard W7-X (large ι) $\longrightarrow$ seen with EUTERPE

Gyrokinetic equation:

$$
\begin{aligned}
\dot{\mathbf{R}}_s &= v_\parallel \mathbf{b} + \frac{m_s}{q_s}\left[\frac{\mu B + v_\parallel^2}{BB^*}\,\mathbf{b}\times\nabla B + \frac{v_\parallel^2}{BB^*}(\nabla\times\mathbf{B})_\perp\right] + \\
&- \frac{q_s}{m_s}\langle A_\parallel\rangle\left\{\mathbf{b} + \frac{m_s}{q_s}\frac{v_\parallel}{BB^*}\left[\mathbf{b}\times\nabla B + (\nabla\times\mathbf{B})_\perp\right]\right\} + \\
&+ \frac{1}{B^*}\mathbf{b}\times\nabla\langle\Psi\rangle
\end{aligned}
$$

$$
\begin{aligned}
\dot{v}_{\parallel,s} &= -\mu\,\nabla B\cdot\left[\mathbf{b} + \frac{m_s}{q_s}\frac{v_\parallel}{BB^*}(\nabla\times\mathbf{B})_\perp\right] + \\
&- \frac{q_s}{m_s}\left\{\mathbf{b} + \frac{m_s}{q_s}\frac{v_\parallel}{BB^*}\left[\mathbf{b}\times\nabla B + (\nabla\times\mathbf{B})_\perp\right]\right\}\cdot\nabla\langle\Psi\rangle
\end{aligned}
$$

with $B^* = B + \frac{m_s v_\parallel}{q_s}\mathbf{b}\cdot(\nabla\times\mathbf{b})$ and $\Psi = \Phi - v_\parallel\langle A_\parallel\rangle$

Note the notation: $v_{\parallel,s} := \frac{1}{m_s}p_{\parallel,s}$ and $\mu := \frac{v_\perp^2}{2B}$

- $\dot{\mathbf{R}}^1$ and $\dot{v_\parallel}^1$ denote the terms in $\dot{\mathbf{R}}$ and $\dot{v}_\parallel$ containing $\Phi, A_\parallel$. The remaining terms are denoted $\dot{\mathbf{R}}^0$ and $\dot{v_\parallel}^0$.
- Splitting:

$$f_s(\mathbf{R}, v_\parallel, \mu) = f_{0,s}(\mathbf{R}, v_\parallel, v_\perp) + \delta f_s(\mathbf{R}, v_\parallel, \mu)$$

- δf equation:

$$\dot{\delta f}_s = -f_{0,s}\left[\dot{\mathbf{R}}_s^1 \frac{\nabla f_{0,s}}{f_{0,s}} + \dot{v}_{\parallel,s}^1 \frac{1}{f_{0,s}}\frac{\partial f_{0,s}}{\partial v_\parallel} + \frac{v_\perp}{2B}\dot{\mathbf{R}}_s^1 \cdot \nabla B \frac{1}{f_{0,s}}\frac{\partial f_{0,s}}{\partial v_\perp}\right]$$

- Maxwellian:

$$f_{0,s} = \frac{n_{0s}(x)}{(2\pi)^{\frac{3}{2}} v_{\mathrm{th},s}^3} e^{-\frac{v_\parallel^2 + v_\perp^2}{2v_{\mathrm{th},s}^2}}, \qquad v_{\mathrm{th},s}^2(x) = \frac{k_B T_s(x)}{m_s}$$

$$\frac{1}{f_{0,s}}\frac{\partial f_{0,s}}{\partial v_{\parallel,\perp}} = -\frac{1}{v_{\mathrm{th},s}^2} v_{\parallel,\perp}, \qquad \frac{1}{f_{0,s}}\nabla f_{0,s} = \frac{1}{n_{0s}}\nabla n_{0s} + \left(-3 + \frac{v_\parallel^2 + v_\perp^2}{v_{\mathrm{th},s}^2}\right)\frac{1}{v_{\mathrm{th},s}}\nabla v_{\mathrm{th},s}$$

Equations in the EUTERPE code III

Field equations:

- Quasineutrality:

$$\sum_s q_s n_s = 0, \qquad n_s = \langle n_s \rangle + \frac{m_s}{q_s} \nabla \cdot \left(\frac{n_{0s}}{B^2} \nabla_\perp \Phi \right)$$

- Adiabatic electrons:

$$n_e = \frac{|e|\, n_{0e}(x)}{k_B T_e} (\Phi - \bar{\Phi})$$

- Ampère's law:

$$-\frac{1}{\mu_0} \nabla_\perp^2 A_\parallel + \sum_s \frac{q_s^2}{m_s} \mathcal{S}[A_\parallel] = \sum_s \langle j_{\parallel,s} \rangle$$

with $\mathcal{S}[A_\parallel] := \int \langle f_0 \langle A_\parallel \rangle \rangle \mathrm{d}W$.
Note: In the code the approximation $\mathcal{S}[A_\parallel] \approx n_{0s} A_\parallel$ is used, giving

$$-\frac{1}{\mu_0} \nabla_\perp^2 A_\parallel + \sum_s n_{0s} \frac{q_s^2}{m_s} A_\parallel = \sum_s \langle j_{\parallel,s} \rangle$$

Pullback formulation: equations

- The corresponding perturbed equations of motion are

$$\dot{\mathbf{R}}^{(1)} = \frac{\mathbf{b}}{B_\parallel^*} \times \nabla \left\langle \phi - v_\parallel A_\parallel^{(\mathrm{s})} - v_\parallel A_\parallel^{(\mathrm{h})} \right\rangle - \frac{q}{m} \langle A_\parallel^{(\mathrm{h})} \rangle \, \mathbf{b}^*$$

$$\dot{v}_\parallel^{(1)} = -\frac{q}{m} \left[\mathbf{b}^* \cdot \nabla \left\langle \phi - v_\parallel A_\parallel^{(\mathrm{h})} \right\rangle + \frac{\partial}{\partial t} \left\langle A_\parallel^{(\mathrm{s})} \right\rangle \right] - \frac{\mu}{m} \frac{\mathbf{b} \times \nabla B}{B_\parallel^*} \cdot \nabla \left\langle A_\parallel^{(\mathrm{s})} \right\rangle$$

- An equation for $\partial A_\parallel^{(\mathrm{s})} / \partial t$ is needed

$$\frac{\partial}{\partial t} A_\parallel^{(\mathrm{s})} + \mathbf{b} \cdot \nabla \phi = 0$$

- Ampere's law takes the form

$$\left(\sum_{s=i,e,f} \frac{\hat{\beta}_s}{\rho_s^2} - \nabla_\perp^2 \right) A_\parallel^{(\mathrm{h})} - \nabla_\perp^2 A_\parallel^{(\mathrm{s})} = \mu_0 \sum_{s=i,e,f} j_{\parallel 1 s}$$

Pullback formulation: numerics

1. At the end of each time step, redefine the magnetic potential splitting:

$$A^{(\mathrm{s})}_{\|(\mathrm{new})}(t_i) = A_\|(t_i) = A^{(\mathrm{s})}_{\|(\mathrm{old})}(t_i) + A^{(\mathrm{h})}_{\|(\mathrm{old})}(t_i)$$

2. As a consequence, redefine $A^{(\mathrm{h})}_{\|(\mathrm{new})}(t_i) = 0$
3. The new mixed-variable distribution function must coincide with its symplectic-formulation counterpart (pullback).

$$f^{(\mathrm{m})}_{1s(\mathrm{new})}(t_i) = f^{(\mathrm{s})}_{1s}(t_i) = f^{(\mathrm{m})}_{1s(\mathrm{old})}(t_i) + \frac{q_s \left\langle A^{(\mathrm{h})}_{\|(\mathrm{old})}(t_i)\right\rangle}{m_s} \frac{\partial F_{0s}}{\partial v_\|}$$

4. Proceed, explicitly solving the mixed-variable system of equations (1)-(8) at the next time step $t_i + \Delta t$ in a usual way, but using Eqs. (1)-(3) as the initial conditions.
5. Perform this rearrangement at each time step.

see:

A Mishchenko, et al. Physics of Plasmas 21 (9), 092110 (2014).
R Kleiber, et al. Physics of Plasmas 23 (3), 032501 (2016)
A Mishchenko, Physics of Plasmas 24 (8), 081206 (2017)

Numerical improvements in EUTERPE code

major progress achieved with:

- Fourier solver successfully tested with pull-back-scheme
- improvement in spline-scheme: parallel gradient discretisation
  ensures consistency in Fourier space
  no parasitic modes
- smoothing at axis of VMEC improved
- interpolation of equilibrium improved
- diagnostics improved (using JULIA and MATLAB)
  two modes fit to frequency and growth rate as standard
  SVD decomposition with iterated frequency refinement

LHD case with $B_0 = 0.619\mathrm{T}$

$T_\mathrm{i} = T_\mathrm{e} = 1\mathrm{keV}, \quad T_\mathrm{fast} = 100\mathrm{keV}, \quad R_0 \approx 3.7\mathrm{m}, \quad N_p = 10$

$< \beta > \approx 3\%$, $\beta_\mathrm{fast}(0) \approx 1.3\%$

iota profile:

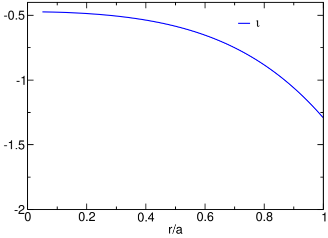

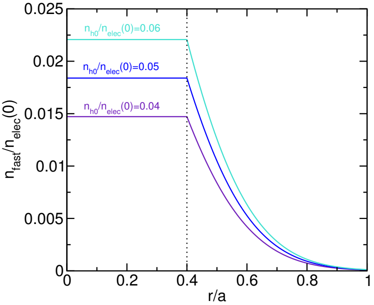

comparison GTC vs. MEGA

D. A. Spong et al.,
Nucl. Fusion **57** 086018 (2017)

- GTC: 3D EM GK turbulence code
- fluid electron model with $E_{||}$ to lowest order in
- markers are not re-inserted: about 40% fast and 7% of thermal ion markers lost
- Gaussian drop-off the fields for the edge and axis boundary condition
- Fourier mode window $m = 1 \dots 8$, $n = 1$

Y. Todo, et al.,
Phys. Plasmas **24**, 081203 (2017)

- MEGA: 3D non-linear resistive MHD code
- +gyro-kinetic fast particles (pressure coupling)
- finite differences, full radius
- numerical resistivity much larger than physical, leads to mode damping

GTC and MEGA results

GTC (Spong et al. 2017):

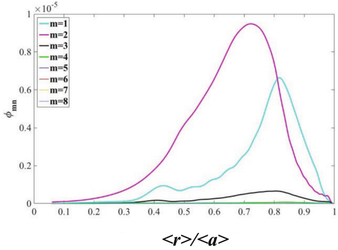

MEGA (Todo et al. 2017):

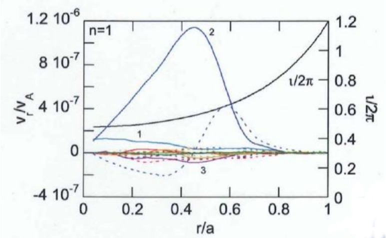

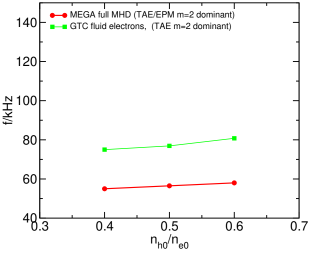

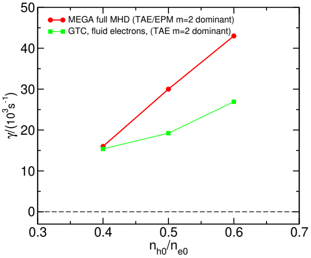

FLUID-EUTERPE: mode structure

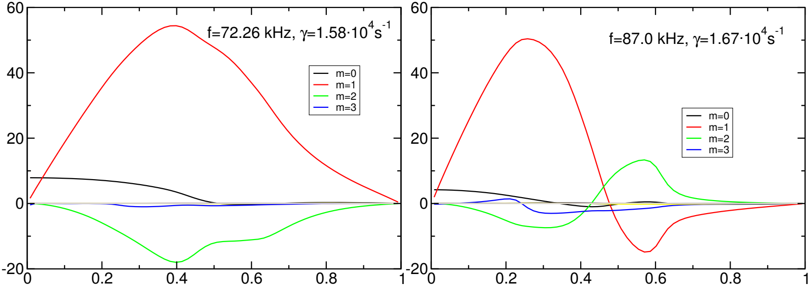

odd TAE, different radial knots

Fluid model:
M. Cole, et al. Plasma Physics and Controlled Fusion 57 (5), 054013.
and M. Borchardt, R. Kleiber and A. Mischhenko 2018 (unpublished)

FLUID-EUTERPE results

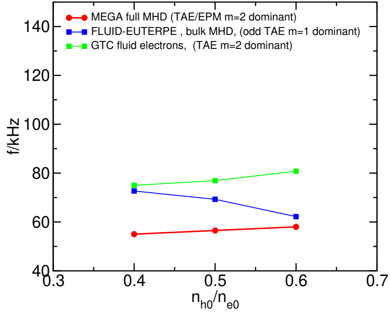

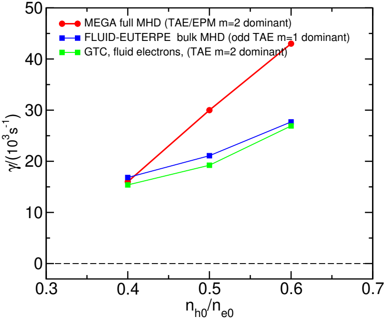

Mode structure

mode B: EAE

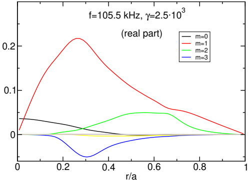

$$\frac{n_h}{n_e} = 0.04$$

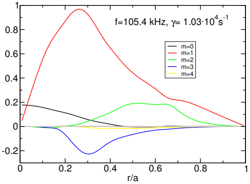

$$\frac{n_h}{n_e} = 0.05$$

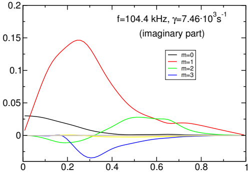

$$\frac{n_h}{n_e} = 0.06$$

mode A: EPM

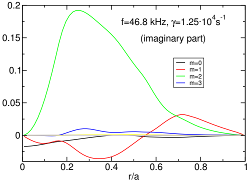

$$\frac{n_h}{n_e} = 0.04$$

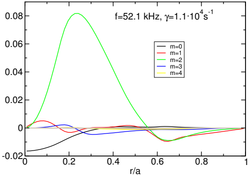

$$\frac{n_h}{n_e} = 0.05$$

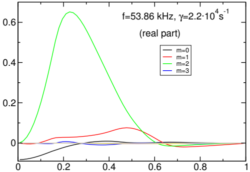

$$\frac{n_h}{n_e} = 0.06$$

note: the frequency measurement at the SVD decomposition and the growth rate estimation from the mode maximum still deviate

EUTERPE gyro-kinetic results

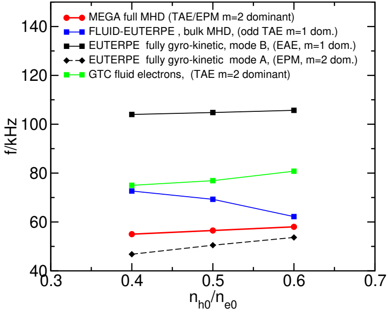

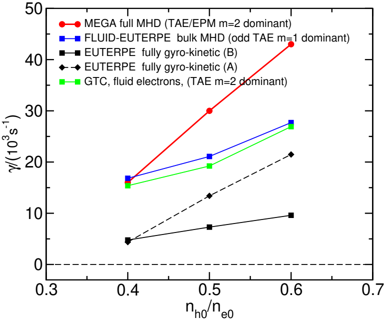

EUTERPE gyro-kinetic results

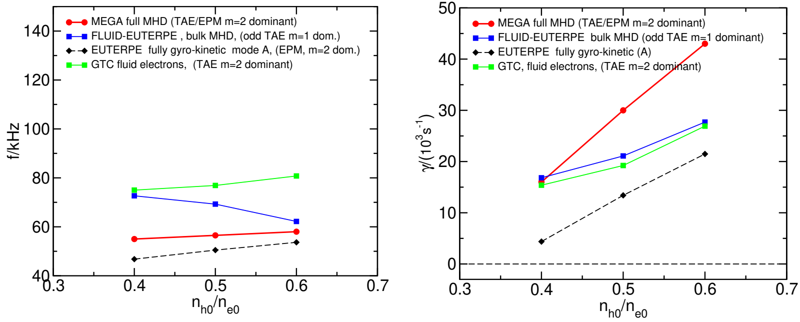

EUTERPE gyro-kinetic results

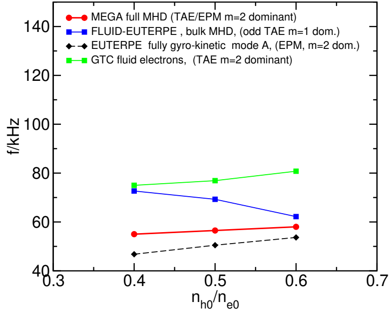

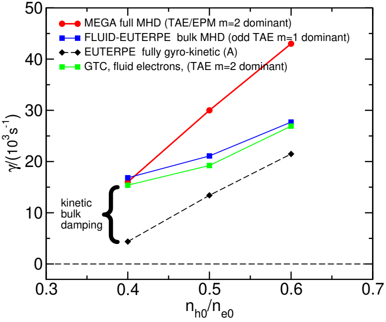

Continuuos spectra and mode location

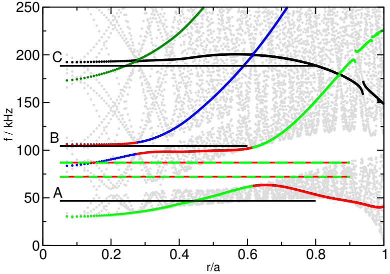

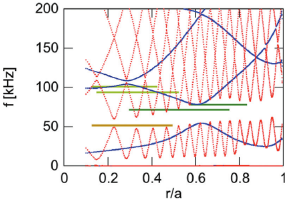

FIG. 5. Alfvén continuous spectra of the toroidal mode number (a) $n = 1$ (blue) and (b) $n = 11$ (red). The frequency and the spatial location of each AE with frequency $f = 52$, 72, 78, 94, 101 kHz are shown with a horizontal line.

CONTI

STELLGAP

with slow sound approximation

Discussion

Alfvén Eigenmodes in LHD

- numerically clean result for $n = -1$
- fully gyro-kinetic results reveal two competing modes: EAE ($m = 1$ dominant) and EPM ($m = 2$ dominant) close to the TAE gap
- EPM agrees approximately with MEGA finding, not regraded missing bulk damping in MEGA
- fluid model FLUID-EUTERPE gives odd TAE
- fluid model GTC gives even TAE
- differences to GTC and MEGA – to be attributed to model differences?
- further investigation but overall agreement satisfying

GAMs in HSX

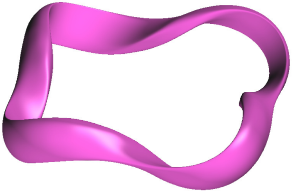

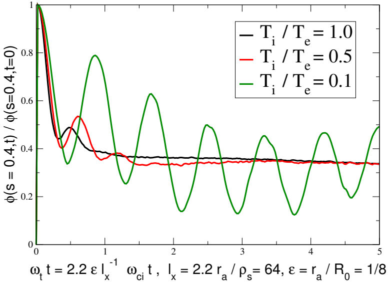

- Low-shear configuration with $\iota = 1/q \approx 1$
- Strong GAM damping:

$$\gamma_{GAM} \sim \exp\left(-\frac{q^2 R^2 \omega_{GAM}^2}{v_{Ti}^2}\right) \ , \ \omega_{GAM}^2 \approx \frac{v_{Ti}^2}{R^2}\left(\frac{7}{4} + \frac{T_e}{T_i}\right)$$

- GAM activity at $T_e \gg T_i$ (similar to OP1.1 W7-X plasma)

Low-iota OP1.2 W7-X

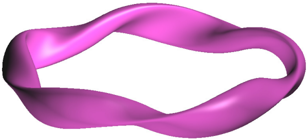

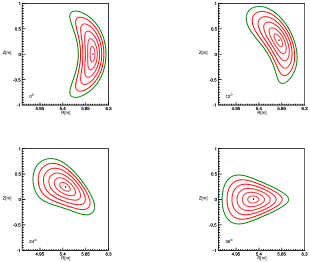

GAMs in low-iota OP1.2 W7-X

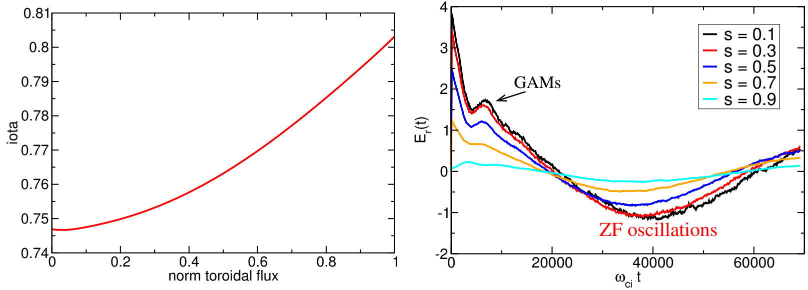

- Rotational transform profile (low-iota OP1.2 finite beta)
- Time traces at different radial positions
- Strong damping of GAMs observed
- Low-frequency zonal flow oscillations

GAMs in W7-X with modified ι

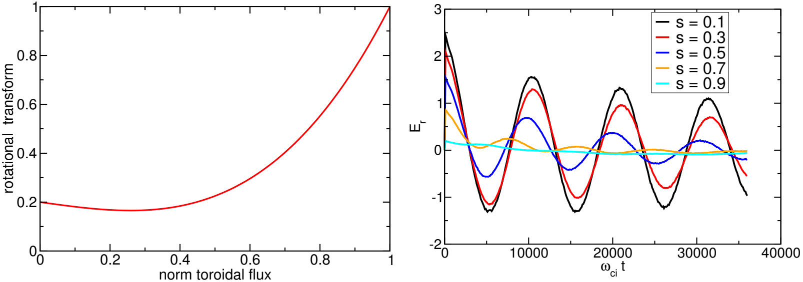

- Modified rotational transform profile (e. g. by ECCD or return currents)
- Time traces at different radial positions
- GAM activity observed
- GAM are weakly damped in the centre (small ι)

QuASDEX (IPP Garching 2030+)

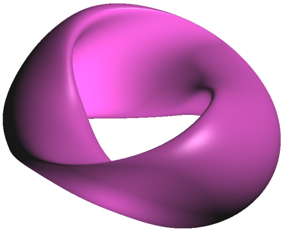

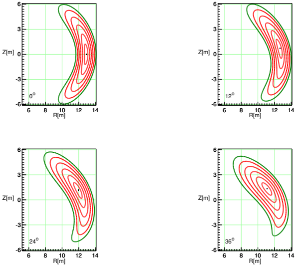

GAM in QuASDEX ($\rho_* \sim 0.005$)

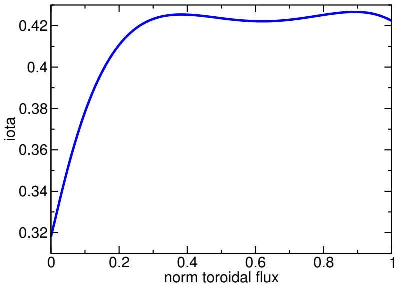

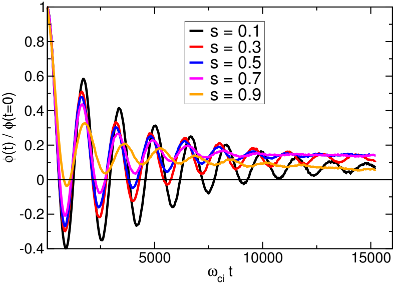

- Rotational transform profile
- Time traces at different radial positions
- GAM activity observed
- GAM are weakly damped in the centre (small ι)

Summary

EUTERPE can go non-linear now and to W7-X

- numerically clean result for $n = -1$ eigenmodes
- three-dimensional with realistic equilibrium
- fully gyro-kinetic, electromagnetic, global *full* radius
- very low mode numbers including $m = 0, 1, \ldots; n = -1$
- no visible pollution with parasitic modes

GAM physics:

- GAMs in HSX for large T_e/T_i; similar to W7-X OP1.1 conditions
- GAMs W7-X with modified ι profile (e. g. by ECCD or return currents)
- GAMs in QuASDEX (IPP Garching 2030+) for $\rho_* \sim 0.005$